

Inclusive prompt $\chi_{c,b}(1^{++})$ production at the LHC

A. G. Shuvaev¹, V. A. Khoze^{1,2}, A. D. Martin^{2,a}, M. G. Ryskin^{1,2}

¹ Petersburg Nuclear Physics Institute, NRC Kurchatov Institute, Gatchina, St. Petersburg 188300, Russia

² Institute for Particle Physics Phenomenology, University of Durham, Durham DH1 3LE, UK

Received: 7 July 2015 / Accepted: 11 December 2015 / Published online: 28 December 2015
© The Author(s) 2015. This article is published with open access at Springerlink.com

Abstract We study the prompt production of the $\chi_c(1^+)$ and $\chi_b(1^+)$ mesons at high energies. Unlike $\chi(0^+, 2^+)$ production, $\chi(1^+)$ mesons cannot be created at LO via the fusion of two on-mass-shell gluons, that is, $gg \rightarrow \chi_{c,b}(1^+)$ are not allowed. However, the available experimental data show that the cross sections for $\chi_c(1^+)$ and $\chi_c(2^+)$ are comparable. We therefore investigate four other $\chi(1^+)$ production mechanisms: namely, (i) the standard NLO process $gg \rightarrow \chi_{c,b}(1^+) + g$, (ii) via gluon virtuality, (iii) via gluon reggeisation and, finally, (iv) the possibility to form $\chi_{c,b}(1^+)$ by the fusion of three gluons, where one extra gluon comes from another parton cascade, as in the Double Parton Scattering processes.

1 Introduction

It is well known that according to the generalised Landau–Yang selection rule a spin-1 meson cannot be produced in the fusion of two identical massless spin-1 particles [1, 2]. Therefore the inclusive $\chi_c(1^+)$ cross section offers the possibility to probe some non-trivial dynamics of the NLO interaction.

There are two ways to overcome the Landau–Yang selection rule: either to account for different virtualities of incoming gluons (that is, to violate their identity) or to consider the formation of $\chi(1^+)$ by three gluons. The third gluon may be emitted as the new secondary particle of the $gg \rightarrow \chi(1^+) + g$ process, or it may occur in the initial state in the process of $g + (gg) \rightarrow \chi$ fusion. Recall that, as shown in [3], the role of such three-gluon mechanisms of J/ψ -meson production increases with energy¹ and may even be dominant at very high energies. Recently the three-gluon J/ψ production was also studied in [4]. Note that, in comparison with the J/ψ , the dynamics of $\chi_c(1^+)$ formation is richer since, due to its

negative C -parity, the J/ψ meson cannot be produced in the fusion of two gluons, even if we account for the different virtualities of these gluons.

The available experimental data on prompt production of χ_c mesons in high-energy hadronic collisions (see [5] for a recent review) concern, as a rule, the transverse momentum p_t distribution of the χ -meson production rates or the ratios of $\sigma(\chi_{c,b}(2^+))/\sigma(\chi_{c,b}(1^+))$ as a function of p_t .² The ratio $R_{21} = \chi(2^+)/\chi(1^+)$ is of the order of one and practically does not depend on p_t . It can be described by a constant, R_{21} , independent of p_t , both for the χ_c and the χ_b processes: in particular for χ_b by the value $R_{21} = 0.85 \pm 0.07$ [6].³ This was not expected. The lowest-order theory predicts the growth of this ratio for decreasing p_t , since, at low p_t , the $\chi(2)$ meson can be produced at LO, while $\chi(1)$ only occurs at NLO (see, for example [8, 9]). Moreover, in fixed-target π -Be interactions at 515 GeV/c the p_t -integrated yields of $\chi_c(1^+)$ ($\sigma = 232 \pm 37 \pm 37$ nb) and $\chi_c(2^+)$ ($\sigma = 407 \pm 71 \pm 69$ nb [10]) were measured. This does not indicate the expected *strong* suppression of $\chi_c(1)$, which cannot be produced at LO via on-mass-shell gluon–gluon fusion. It is worth mentioning that new important information could come from fixed-target experiments using an LHC beam, as advocated in [11], where lower p_t values could be reached. Thus it is topical to study theoretically the different possible mechanisms of $\chi(1)$ production.

¹ Unfortunately there was a confusion in [3] – for the three-gluon mechanism the cross section, and not the amplitude, grows as $\ln s$. Thus the cross section at LHC energies will be a few times smaller.

^a e-mail: a.d.martin@durham.ac.uk

² Experimentally it is easier to measure such ratios since various theoretical and experimental uncertainties cancel out. As far as we are aware, currently there are no high-energy data at low p_t and no data on the rapidity distribution $d\sigma/dy$ or on the total cross sections for $\chi_{c,b}(1)$ except for the relatively low-energy data in π -Be collisions. Note that the p_t of the J/ψ and not that of χ_c is measured, but due to the large J/ψ mass (close to the χ_c mass) the p_t of J/ψ is rather close to that of χ_c , and qualitatively reproduces well the behaviour with respect to the p_t of χ_c .

³ Note that there is an indication for an increase of the ratio R_{21} at low p_t in the LHCb measurement of χ_c at 7 TeV [7]. Therefore it is desirable that the LHCb collaboration perform a new measurement of this ratio at low p_t during run-II of the LHC.

The inclusive cross sections were calculated at lowest order in [12, 13]. Numerical evaluations at the LHC energy are given, for example, in [8, 9]. A specific higher-order process, the so-called ‘ s -channel $Q\bar{Q}$ -cut’ was considered in [14–16]. For a more detailed review see, for example, [17].

In the present paper we discuss all the different possibilities of colour-singlet $\chi_c(1^+)$ and $\chi_b(1^+)$ inclusive production. We will not discuss here the colour-octet contribution, in particular, since at the moment the importance of colour-octet contributions to the $\chi_c(1, 2)$ production remains open; see for instance [5, 17–19]. Note that Ref. [18] presents the complete NLO NRQCD predictions for the polarised $\chi_c(1, 2)$ production at medium and high p_t , which when compared to forthcoming LHC measurements could allow a detailed probe of the validity of NRQCD and the colour-octet mechanism.

We consider the lowest α_s -order process and, moreover, if in some kinematical domain we find that the cross section is enhanced by a large logarithm (either of virtuality, $\ln q^2$, or of energy, $\ln s$), then we will focus on this leading logarithm (LL) contribution. We emphasise that the aim of the paper is not to present a precise quantitative prediction,⁴ but rather to compare the role of different mechanisms of $\chi(1^+)$ production in high-energy hadron–hadron collisions.

We note that χ_b production has advantages over χ_c both from the theoretical and experimental viewpoints. Due to the larger mass of χ_b (i) the perturbative QCD approach is better justified and (ii) it is easier to detect the more energetic decay products.

In Sect. 2 we first consider the cross section caused by the $gg \rightarrow \chi(1^+) + g$ subprocess, and second due to the different virtualities of two incoming gluons. Then in Sect. 3 we discuss the production via three-gluon fusion where a pair of t -channel gluons represents the reggeisation of one incoming gluon. Next, in Sect. 4 we study a most interesting possibility when the two gluons come from two different parton cascades. This mechanism for $\chi(1^+)$ production has not been studied before. At asymptotically high energy this should be the dominating contribution. An interesting fact is that in such a case the cross section in the central region is expected to be smaller than that near the proton fragmentation domain. We give our conclusions in Sect. 5.

2 Lowest-order $\chi(1^+)$ production

In this section we study production by the two-gluon initiated states shown by ‘1 and 2’ in Fig. 1. We show separately the contribution where all three gluons couple to the heavy quark loop (Fig. 1a), and the contribution where only two t -channel gluons couple to the heavy quark loop (Fig. 1b) which may not vanish for $\chi(1^+)$ if the virtualities of these

two gluons are different (Fig. 1b). This contribution may be considered separately and formally is called ‘production’ via two-gluon fusion. However, actually this is just part of the whole $gg \rightarrow \chi(1^+) + g$ cross section.

Another point is that it is natural to consider for this part the role of t -channel gluon reggeisation, which is the simplest example of $\chi(1^+)$ production via three-gluon fusion $g + (gg) \rightarrow \chi(1^+)$. For this reason we will describe the contribution of Fig. 1b in more detail in Sect. 2.2, and the reggeisation in Sect. 3.

Finally, in Fig. 1c we show the process initiated by a highly virtual s -channel gluon.

2.1 The $gg \rightarrow \chi(1^+) + g$ process

The simplest possibility to overcome the Landau–Yang selection rule is to create the $\chi(1^+)$ meson together with an additional gluon. The corresponding ‘hard’ cross section was calculated in [12, 13]

$$\frac{d\hat{\sigma}(gg \rightarrow \chi(1^+) + g)}{dt} = \frac{12\pi\alpha_s^3 R'^2}{M^3 s^2} \cdot \frac{P^2[M^2 P^2(M^4 - 4P) + 2Q(-M^8 + 5M^4 P + P^2) - 15M^2 Q^2]}{(Q - M^2 P)^4} \quad (1)$$

where s, t, u are the Mandelstam variables for the hard subprocess. The quantities $P = st + su + ut$ and $Q = stu$; and M is the $\chi_c(1^+)$ or $\chi_b(1^+)$ meson mass.

In Eq. (1) the non-relativistic wave function of the meson is assumed. The derivative of the P -wave function at the origin is denoted R' . In our calculations for $\chi_c(1^+)$ we use the values $R'^2/M^2 = 0.006 \text{ GeV}^3$ (as in [12, 13]) and the QCD coupling $\alpha_s = 0.335$, which provide reasonable widths of the $\chi_c(0, 1, 2)$ mesons calculated accounting for the α_s corrections (see e.g. [20]). For $\chi_b(1^+)$ we take $R'^2 = 1 \text{ GeV}^5$ similar to that in [8, 9], which is consistent with the potential model results, and $\alpha_s = 0.22$ corresponding to the higher scale appropriate for χ_b production.

In comparison with the natural parity $\chi_c(0^+)$ and $\chi_c(2^+)$ mesons, which can be formed via on-mass-shell gluon–gluon fusion with the cross section $\hat{\sigma} \propto \alpha_s^2$, the cross section (1) contains an extra power of the QCD coupling (not accompanied by any large logarithm). Therefore $gg \rightarrow \chi(1^+) + g$ can be considered as a NLO production process.

Expression (1) has to be convoluted with the incoming parton distributions and integrated over t and s . Since we are looking for the inclusive $\chi(1^+)$ production we fix the rapidity, Y , of $\chi(1^+)$ meson and choose to integrate over the variables y and p_t , where p_t is the transverse momentum of the final gluon while y is the rapidity separation between this gluon and the $\chi(1^+)$ meson. It is easy to check that the corresponding Jacobian $J = 1$ (see e.g. [21]). Thus the cross section of $\chi(1^+)$ production in proton–proton collisions reads

⁴ Precise results would require dedicated higher-order calculations.

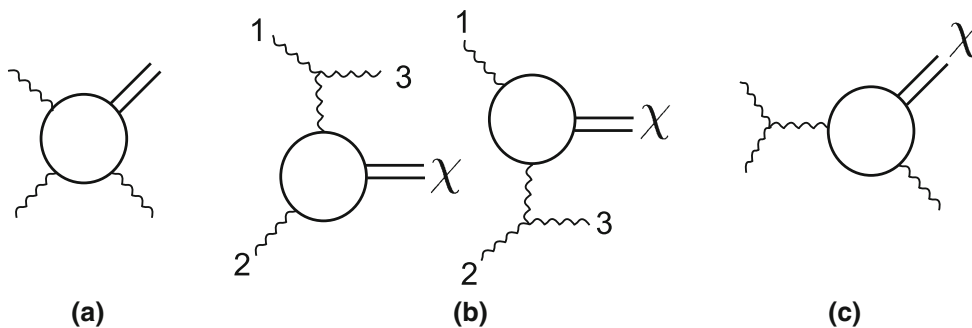


Fig. 1 Subprocesses for $\chi(1^+)$ production: **a** the standard $gg \rightarrow \chi(1^+) + g$ process where three on-mass-shell gluons couple to the heavy quark loop; **b, c** where one virtual gluon and one on-mass-shell

gluon couple to the heavy quark loop – the virtual gluon has $q^2 < 0$ for **b** and $q^2 > 0$ for **c**

$$\frac{d\sigma}{dY} = \int x_1 g(x_1, \mu_F) \frac{d\hat{\sigma}(gg \rightarrow \chi(1^+) + g)}{dt} \times x_2 g(x_2, \mu_F) dy dp_t^2, \tag{2}$$

where $g(x, \mu_F)$ is the density of gluons which carry a fraction x of the momentum of the incoming proton (measured at factorisation scale μ_F). We have the variables

$$x_{1,2} = (m_t + p_t e^{\pm Y}) e^{\pm Y} / \sqrt{s} \tag{3}$$

where $m_t^2 = M^2 + p_t^2$. The hard cross section $d\hat{\sigma}/dt$ is given by (1) with

$$s = m_t^2 + p_t^2 + m_t p_t (e^Y + e^{-Y}), \tag{4}$$

$$t = -p_t^2 - m_t p_t e^Y, \tag{5}$$

$$u = -p_t^2 - m_t p_t e^{-Y}. \tag{6}$$

The expected cross section is shown in Table 1 where the LO MSTW2008 [22] PDFs were used.

2.2 Production via $g^* + g \rightarrow \chi(1^+)$ fusion

Here we consider the possibility of $\chi(1^+)$ production via ‘virtual+real’ gluon fusion processes,⁵ which are shown in Fig. 1. These processes are not forbidden thanks to the different mass/virtualities of the initial gluons. The corresponding ‘hard’ cross section can be extracted from (1) using the ‘equivalent photon/gluon’ approximation [24,25]. Indeed, in the limit of $s \gg M^2, |t|$, the dominant contribution comes from a diagram where first the incoming gluon with momentum, say, p_1 emits the final gluon p_3 and then the virtual gluon, g^* , with momentum $q = p_1 - p_3$ interacts with another incoming (quasi-real) gluon p_2 to produce the $\chi(1^+)$ meson.⁶

⁵ The production via $g^* + g$ fusion was discussed in detail in [23].

⁶ Recall that in terms of the unintegrated gluon density $f_g(x, q_t, \mu_F)$ the value of $xg(x, \mu_F)$ is given by the logarithmic integral $xg(x, \mu_F) = \int^{\mu_F} f_g(x, q_t, \mu_F) dq_t^2/q_t^2$. That is, each function xg contains a large logarithm. In this logarithmic integration the virtuality of the initial

Thus in the large s limit we may write the cross section (1) as the product of the virtual gluon flux, $dN = (\alpha_s N_c / \pi) (dz/z) dq^2/q^2$ times the elementary $g^* + g \rightarrow \chi(1^+)$ cross section. That is

$$\frac{d\hat{\sigma}}{dt} \Big|_{s \gg M^2, |t|} = \frac{dN}{dq^2} \hat{\sigma}(g^* + g \rightarrow \chi_c(1^+)). \tag{7}$$

(The factor dz/z in dN corresponds to the integration over the rapidity separation y and is omitted here.) In this way we get

$$\hat{\sigma}(g^* + g \rightarrow \chi(1^+)) = \frac{4\pi^2 \alpha_s^2 R'^2}{M^3} |t| \frac{4M^2 - 2t}{m_t^8}, \tag{8}$$

where the virtuality, q^2 , of off-mass-shell gluon g^* plays the role of $t = q^2$ in (1).

Since the elementary cross section (8) vanishes as $q^2 \rightarrow 0$, we cannot consider the incoming gluon, with momentum q , as an on-mass-shell parton. The inclusive cross section should therefore be written in terms of the *unintegrated* gluon density which is defined in such a way that

$$xg(x, \mu_F) = \int^{\mu_F} f_g(x, q^2, \mu_F) \frac{dq^2}{q^2}. \tag{9}$$

Thus we obtain

$$\frac{d\sigma}{dY} = \int x_1 g(x_1, \mu_F) \hat{\sigma}(g^* + g \rightarrow \chi(1^+)) f_g(x_2, q^2, \mu_F) \frac{dq^2}{q^2} + (x_2 \leftrightarrow x_1), \tag{10}$$

with $x_{1,2} = e^{\pm Y} \sqrt{(M^2 - q^2)/s}$.

Note that the dq^2/q^2 integral does not now have a logarithmic structure since the ‘hard’ cross section (8) contains a

Footnote 6 continued
gluon is small, $q^2 \sim q_t^2 \ll \mu_F^2$. So this gluon may be considered as an on-mass-shell particle.

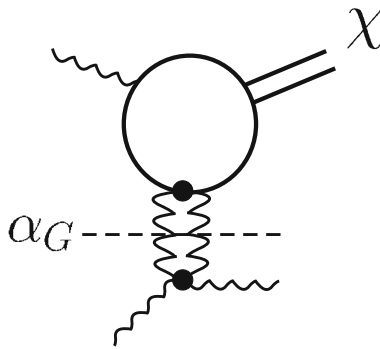


Fig. 2 $\chi(1^+)$ production via the fusion of an incoming gluon with a pair of gluons which form a Regge trajectory α_G

factor $t = q^2$. In other words Eq. (10) should be considered as a NLO contribution (in comparison with LO $\chi(0^+, 2^+)$ meson production) at the same level as the cross section (2). Moreover, it should not be considered as a new contribution – it is just a part of the whole cross section (2).

The value of contribution (10) shown in Table 1 is obtained by calculating the unintegrated gluon density starting from the MSTW2008 [22] PDFs based on the KMR/MRW last-step prescription [26, 27]. In this prescription we have used the LO splitting functions but kept the more exact NLO kinematics. As it was shown in [27] this provides an accuracy close to that given by the NLO prescription. Note that here we have used the gluons unintegrated over the virtuality, q^2 , and not over the transverse momentum squared, q_t^2 (see [27] for details).

The contributions (2) and (10) were evaluated using the MSTW2008 LO PDFs for the integrated gluons xg . For the very low $q^2 < Q_0^2$ we assume the saturation-like behaviour $xg(x, q^2) = xg(x, Q_0^2)(q^2/Q_0^2)$.

3 Production via gluon reggeisation

An attractive possibility to organise the fusion of one gluon with the pair of incoming gluons, that is, the $g + (gg) \rightarrow \chi(1^+)$ subprocess, is to consider the contribution coming from gluon reggeisation; see Fig. 2. On one hand the gluon trajectory is described by the diagrams where the initial t -channel gluon is replaced by the exchange of two t -channel gluons. On the other hand this contribution is enhanced by large logarithms of the proton–proton energy, or to be more precise, by a $1/\omega_0$ factor, where ω_0 denotes the shift of the position of the BFKL vacuum singularity $\alpha_{\text{BFKL}} = 1 + \omega_0$. Recall that thanks to the bootstrap condition [28–30] if we account for the gluon trajectory then we include *all* the contributions (of the antisymmetric colour-octet states, which are of interest here) enhanced by the $1/\omega_0$ factor, that is – by the large leading logarithm of the energy.

Let us explain in more detail how the gluon trajectory is built up. Consider the diagrams where the additional t -channel gluon is added to the usual ladder diagram (inside the same parton cascade). The simplest such diagram (in Feynman gauge) is where the additional gluon is between the χ_c and the nearest s -channel gluon of the ladder (that is, between the c -quark loop and gluon 3 in Fig. 1b). The contribution of this diagram is enhanced by two logarithms. One logarithm, $\ln q^2$, comes from the integration over the k_t of the new t -channel gluon. The other logarithm comes from the integration over the longitudinal component of the new gluon’s momentum, which corresponds to the integration over the mass of the intermediate s -channel gluon which emits the new t -channel gluon. This longitudinal logarithm is actually equal to the rapidity separation between the χ_c meson and the nearest s -channel gluon. This rapidity separation is driven by the intercept (the x -dependence) of the parton cascade. In the BFKL approach this logarithm is equal to $1/\omega_0$. Moreover, in terms of the BFKL amplitude, the coherent sum of such diagrams (where the new t -channel gluon couples to the different s -channel gluons in the ladder) is described by the gluon trajectory

$$\alpha_G(q^2) = \frac{\alpha_s N_c}{2\pi} \ln q^2. \quad (11)$$

Note that in this approach (just as in two-gluon fusion $g^* + g \rightarrow \chi_c(1^+)$) the corresponding contribution vanishes when the ‘reggeised’ gluon virtuality $q^2 \rightarrow 0$. Indeed, due to gauge invariance, the whole set of diagrams which describe gluon reggeisation can be reduced to a one-gluon loop inserted in the place of the original gluon propagator (see, for example [31]). Thus the result looks like cross section (10) multiplied by the gluon trajectory $\alpha_G(q^2)$ and by the $1/\omega_0$ factor.

Moreover, contrary to inclusive J/ψ production (where the gluon pair should be in a symmetric colour-octet state and the analogous contribution is imaginary), in the case of $\chi(1^+)$ we deal with the *antisymmetric* colour octet – that is, with a true gluon trajectory of negative signature. Therefore the logarithmically enhanced contribution is real and *interferes* with the lowest α_s -order $g^* + g \rightarrow \chi_c(1^+)$ amplitude considered in the previous section.

Thus, finally, to lowest order in α_s , the cross section (10) should be multiplied by a ‘double logarithmic’ factor A , where

$$A = \left[1 + 2 \frac{\alpha_s N_c}{2\pi \omega_0} \ln(q_1^2/q_2^2) \right]. \quad (12)$$

Here the q^2 logarithm comes from the integration over the transverse momentum k_t in the loop corresponding to the gluon trajectory. In the region of $k_t^2 \ll q^2$, the integral takes the form

$$\int^{q^2} \frac{dk_t^2}{k_t^2} \tag{13}$$

Note that the amplitude for unnatural parity 1^+ meson production

$$g(q_1) + g(q_2) \rightarrow \chi(1^+) \tag{14}$$

is antisymmetric with respect to the permutation of the two gluons. Therefore in the amplitude (14) we have the logarithm of the ratio q_1^2/q_2^2 . This result solves the problem of the infrared cutoff at low k_t in the integral (13). In the pure symmetric configuration (with $q_1^2 = q_2^2$) we get zero. This fact in some sense is similar to the Landau–Yang selection rule – a spin 1^+ particle cannot decay into two identical transverse gluons.⁷

Recall that in the case of $\chi(1^+)$ production the second t -channel gluon (whose distribution is written here in terms of the ‘gluon reggeisation’ trajectory (11)) is not a virtual loop correction to the main amplitude. Rather, this is a particular new channel to produce a spin 1^+ meson. For this reason it should not be combined with the real, s -channel gluon emission. The infrared divergence in (12) is cancelled between the diagrams with the upper (q_1) and the lower (q_2) gluon insertions; and not between the virtual loop (reggeisation) and the real gluon emission.⁸

The results of the numerical estimate of the corresponding order of α_s contribution⁹ are presented in the fourth column of Table 1. Here we have used the value of $\omega_0 = 1/4$, which is close to that expected for the BFKL pomeron after the resummation of the next-to-leading log corrections [32–34]. Recall that at the lowest α_s order, the ‘reggeised induced’ contribution is proportional to α_s/ω_0 . We choose reasonable values of ω_0 and α_s to indicate the possible size of the effect.

As expected, the result is negative, since at $q^2 < 0$ the gluon trajectory is shifted to lower values of $\alpha_G(q^2) < 1$. However, due to the cancellation between the q_1 and q_2 terms the whole contribution is not too large in spite of the $1/\omega_0$ enhancement.

Recall, however, that at the present stage we account for the order of α_s reggeised correction only. When the ‘correction’ becomes large the higher-order α_s terms become

⁷ Recall that as we are looking for the leading logarithm the gluons may be considered as quasi-real, transverse particles.

⁸ Just as in the case of the colourless Higgs boson production, the infrared divergence caused by real emission is cancelled by the true reggeisation diagram where (in Feynman gauge) the additional t -channel gluon couples to the s -channel gluons above and below the colourless boson.

⁹ The contribution of the terms $\alpha \ln q_1^2$ and $\alpha \ln q_2^2$ are calculated separately. In the first case the gluon q_1 is written in terms of the unintegrated distribution, f_g , while for gluon q_2 we may use the integrated gluon distribution $x_2g(x_2, \mu_F)$, and vice versa.

Table 1 The cross section $d\sigma/dY$ in μb for producing $\chi_c(1^+)$ by the various mechanisms at 7 (13) TeV. Note that the $g^*g \rightarrow \chi$ is already included in the $gg \rightarrow \chi + g$ contribution and has only to be considered separately to facilitate the study of the Regge contribution

Y	$gg \rightarrow \chi + g$	$g^*g \rightarrow \chi$	G -regge	DPS
0.0	9.8 (17.2)	6.3 (10.5)	0.0 (0.0)	1.1 (2.2)
1.0	9.5 (16.8)	6.2 (10.3)	−1.0 (−1.3)	1.2 (2.4)
2.0	8.7 (15.6)	5.6 (9.6)	−1.9 (−2.5)	1.4 (2.9)
3.0	7.4 (13.7)	4.7 (8.5)	−2.5 (−3.3)	1.7 (3.6)
4.0	5.6 (11.3)	3.6 (7.1)	−2.9 (−3.8)	2.1 (4.7)
5.0	3.6 (8.5)	2.1 (5.4)	−2.9 (−4.1)	2.3 (5.9)
6.0	1.5 (5.1)	0.6 (2.9)	−2.4 (−4.5)	1.8 (4.6)

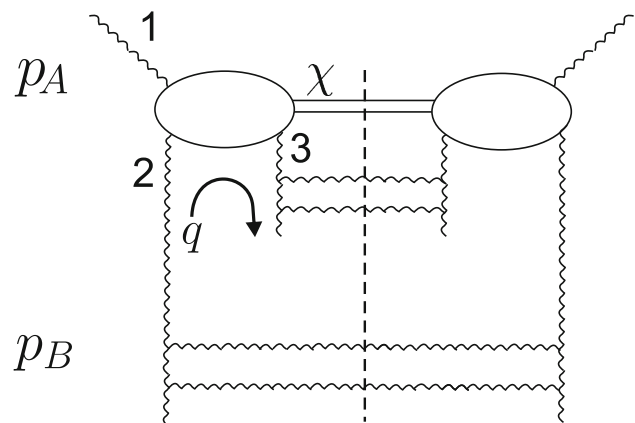


Fig. 3 The diagram for the cross section for $\chi(1^+)$ production via the fusion of two gluons from different parton cascades, where p_A and p_B are the four momenta of the incoming protons (not shown). The diagram is for the cross section, AA^* , so the particles intersected by the dashed line are on-mass-shell

important replacing effectively the first and negative α_s contribution (let us denote it as $-\delta_R$) by the positive exponential factor like $\exp(-\delta_R)$.

4 Production via two parton cascades

Here we consider the situation when all three (quasi-real) gluons couple to the heavy quark loop directly. The most interesting possibility is to form the incoming (gg) pair taking the two gluons from two different parton cascades; see Fig. 3. The probability to find the corresponding pair is given by the product of the gluon densities, $x_1g(x_1) \times x_2g(x_2)$, multiplied by the probability that the two cascades overlap in transverse space. Since in the low x region (which is relevant at high energies) the parton density grows as a power of $(1/x)$ – that is $xg(x) \propto x^{-\lambda}$ – this contribution will dominate asymptotically at very high energies.

In double parton scattering (DPS) the probability of cascade overlap in transverse space is given by a factor $1/\sigma_{\text{eff}}^{\text{DPS}}$ (see e.g. [35,36]), where

$$\frac{1}{\sigma_{\text{eff}}^{\text{DPS}}} = \int F^4(q^2) \frac{d^2q}{4\pi^2}. \tag{15}$$

Actually this factor results from the integration (15) over the ('pomeron') loop formed by the two gluon cascades. The integral is driven by the proton form factor $F(t)$, that is, by the $t \simeq q^2$ dependence of the proton–pomeron vertex. However, while for DPS the loop contains four form factors (leading to F^4 in (15)) in our case we have only two form factors (we need two cascades on one side of Fig. 3 only). Therefore (assuming exponential dependence) we have

$$\sigma_{\text{eff}}^\chi = \frac{1}{2} \sigma_{\text{eff}}^{\text{DPS}}. \tag{16}$$

We emphasise that the typical value of $|t|$ in the pomeron loop integration simultaneously plays the role of the lower limit for the factorisation scale, μ_F^2 . In terms of $\sigma_{\text{eff}}^{\text{DPS}}$ (and assuming the exponential t -behaviour) this limit is $\mu_F^2 > \langle |t| \rangle = 4\pi/\sigma_{\text{eff}}^{\text{DPS}}$.

Let us denote the momenta of the three gluons as k_i ($i = 1, 2, 3$). In terms of the incoming proton's momenta, p_A and p_B , we may write

$$k_1 \simeq \alpha p_A + k_{1t}, \tag{17}$$

$$k_i \simeq \beta_i p_B + k_{it} \quad \text{for } i = 2, 3. \tag{18}$$

To calculate the corresponding matrix element we use the gauge invariance condition ($\mathcal{M}_\mu k_\mu = 0$) and replace the proton's momenta p_A, p_B transferred through the spin part (or numerator) of the gluon's propagators by k_{1t}/α and k_{it}/β_i , respectively. Note that in order to keep the leading (DGLAP) logarithms in the k_t integrals we retain the lowest power of k_{it} in the matrix element.¹⁰

Thus the matrix element for $ggg \rightarrow \chi(1^+)$, corresponding to the heavy quark loop in Fig. 3, takes a rather simple form,

$$\mathcal{M} = -i B f^{abc} \frac{A_s g^3}{N_c M}, \tag{19}$$

where f^{abc} is the antisymmetric colour tensor, $N_c = 3$ is the number of colours, and g is the QCD coupling ($\alpha_s = g^2/4\pi$). The basic amplitude A_s contains a spin part (given by the trace around the quark loop) and a part corresponding to the propagator poles. It is of the form

$$A_s = 16(a_1 z_1 + a_2 z_2) \tag{20}$$

where the trace gives

¹⁰ Together with the denominators ($1/k_i^2$) of the gluon propagators this will give in the cross section the logarithm $\int k_{it}^2 d^2 k_{it} / k_i^4$.

$$a_1 = (e_a \cdot k_{3t}) \epsilon_{\alpha\beta\gamma\delta} k_{2t}^\alpha p_A^\beta p_B^\gamma e_\chi^\delta, \tag{21}$$

$$a_2 = (e_a \cdot k_{2t}) \epsilon_{\alpha\beta\gamma\delta} k_{3t}^\alpha p_A^\beta p_B^\gamma e_\chi^\delta, \tag{22}$$

and the poles are

$$z_1 = \frac{2\alpha\beta_{23} s}{\alpha(2z - 1)\beta_{23}s - |\vec{k}_{1t} - \vec{k}_{2t}|^2 - M^2}, \tag{23}$$

$$z_2 = \frac{2\alpha\beta_{23} s}{\alpha\beta_{23}s(1 - 2z) - |\vec{k}_{1t} - \vec{k}_{2t}|^2 - M^2}, \tag{24}$$

where the denominators include the contribution of the longitudinal ($\alpha\beta_{23}s(1 - 2z)$) and transverse ($-|\vec{k}_{1t} - \vec{k}_{2t}|^2$) components of the square of the momentum. Here e_χ and e_a are the $\chi(1^+)$ and k_1 -gluon polarisation vectors. Also we have introduced the relative momentum fraction $z = \beta_2/(\beta_2 + \beta_3)$, where

$$\beta_{23} = \beta_2 + \beta_3 = (M^2 + |\vec{k}_{1t} + \vec{k}_{2t}|^2)/\alpha s. \tag{25}$$

The value of β_{23} is fixed by the $\chi(1^+)$ meson mass and its rapidity. Finally, the normalisation constant B in (19) is given by

$$B = \sqrt{\frac{3R'^2}{\pi M^3}}. \tag{26}$$

Recall that in the diagram for the cross section, Fig. 3, we have four t -channel gluons from the proton p_B side.¹¹ These four gluons form three loops of integration. The integrals over the transverse momenta components have already been discussed: two loops give the logarithmic integrals $\int k_{it}^2 d^2 k_{it} / k_i^4$ corresponding to the gluon PDF given by the parton cascade i , while the third integral (over t) is limited by the proton form factor. The longitudinal momentum component in the central loop is fixed by the condition that the $\chi(1^+)$ meson (and other secondary partons) should be on-mass-shell. Finally, we have the loop integrations over the gluon longitudinal momentum in each amplitude, A and A^* . These integrals can be written in terms of z and can be closed on the quark pole;¹² that is, in our non-relativistic approximation (for the $\chi(1^+)$ wave function) we get an intermediate

¹¹ In general, there may be a diagram where the gluon pair (gg) goes in the p_B direction in one amplitude, A , but goes in the other, p_A , direction in the amplitude A^* . Such a contribution either corresponds to the three-gluon singularity (in the ω plane) which has a lower intercept ($\omega_0 \sim 0$ or even negative – this contribution is small): or, dealing with the BFKL pomeron, we have to consider this (gg) pair as gluon reggeisation which (in the lowest α_s order) was already considered in Sect. 3.

¹² In general, in our case with a $L = 1$ wave function, some part of the contribution may contain poles of second order (see e.g. [37]). However, as far as we keep just the leading logarithms in k_t , that is, the lowest power of k_t , the residue of these second-order poles vanishes at $z = 0$ or $z = 1$. Therefore actually we deal only with simple first-order poles.

state with both quarks on-mass-shell. The pole position is

$$z = \frac{2(\vec{k}_{2t} \cdot \vec{k}_{3t})}{M^2}. \tag{27}$$

So, finally, the matrix element (19) reads

$$\mathcal{M} = 32\pi B f^{abc} \frac{g^3(a_1 + a_2)}{N_c M}. \tag{28}$$

To obtain the cross section we have to sum over the $\chi(1^+)$ polarisations, e_χ , average over e_a and integrate over the gluon transverse momenta. A problem is that according to (27) the value of z depends on these momenta and we cannot use the usual, integrated PDFs; each value of k_{it} corresponds to its own z . Therefore we have to use the unintegrated distribution in the same way as described in Sect. 2.2. Moreover, in our calculation we have to keep only the poles with the positive $z < 1$. Otherwise one of the gluons (z or $1 - z$) will have a negative energy and so must be considered as an outgoing and not an incoming particle. Such a configuration describes the $gg \rightarrow \chi(1^+) + g$ subprocess which has already been discussed in Sect. 2.

Thus the ‘DPS’ component of the inclusive $\chi(1^+)$ cross section (which we call σ^{DPS}) reads

$$\begin{aligned} \frac{d\sigma^{\text{DPS}}}{dY} &= \frac{\pi^3 \alpha_s^3 R'^2}{\sigma_{\text{eff}}^{\text{DPS}} M^9} \frac{32}{9} \int^{M^2} \frac{dk_{2t}^2}{k_{2t}^2} \frac{dk_{3t}^2}{k_{3t}^2} \alpha g(\alpha, M^2) \\ &\cdot \int_0^{2\pi} \frac{d\phi}{2\pi} (1 + \cos^2 \phi) f_g(x_2 = \beta_{23}(1 - z), k_{2t}^2) \\ &\times f_g(x_3 = z\beta_{23}, k_{3t}^2) \Theta(z) \Theta(1 - z) + (\alpha \leftrightarrow \beta_{23}), \end{aligned} \tag{29}$$

where z is given by (27) and where we take the factorisation scale $\mu_F = M$. Since, within the Leading Logarithm approximation, both $k_{1t}^2, k_{2t}^2 \ll M^2$, we may replace in the first argument of $f_g(\beta_{23}(1 - z), \dots)$ the value of $(1 - z)$ by 1, that is, $f_g(\beta_{23}(1 - z), \dots)$ becomes $f_g(\beta_{23}, \dots)$. The origin of $\cos^2 \phi$ in the cross section comes from the convolution of a_1 and a_2 .

The predicted ‘DPS’ part of the $\chi(1^+)$ production cross section is presented in the fifth column of Table 1. In the numerical calculation we have used MSTW2008LO partons [22] and $\sigma_{\text{eff}}^{\text{DPS}} = 10 \text{ mb}$ [38, 39].

5 Discussion

As seen from Tables 1 and 2, in the central rapidity region ($Y = 0$) the main contribution to $\chi(1^+)$ production comes from the most trivial $gg \rightarrow \chi(1^+) + g$ subprocess, even at 13 TeV. This contribution decreases with $|Y|$, that is, towards the edges of the available rapidity space.

Table 2 The cross section $d\sigma/dY$ in nb for producing $\chi_b(1^+)$ by the various mechanisms at 13 TeV. Note that the $g^*g \rightarrow \chi$ is already included in the $gg \rightarrow \chi + g$ contribution, and has only to be considered separately to facilitate the study of the Regge contribution

Y	$gg \rightarrow \chi + g$	$g^*g \rightarrow \chi$	G -regge	DPS
0.0	37	30	0	2.2
1.0	36	29	-10	2.4
2.0	31	25	-18	2.7
3.0	24	18	-22	3.1
4.0	16	11	-23	3.1
5.0	8	3	-18	2.4

The expected correction due to gluon reggeisation vanishes at $Y = 0$, in accord with the generalised Landau–Yang selection rule, which is valid for the symmetric configuration. Moreover, for $Y \neq 0$ it is negative, and at large rapidity Y it becomes quite large in comparison with the original (without reggeisation) contribution. The absolute value of the Regge contribution increases with $|Y|$ (up to $Y \sim 5$) making the overall rapidity (Y) distribution a bit narrower. We emphasise, however, that the results of Tables 1 and 2 are presented just for illustration purposes, and include the $\mathcal{O}(\alpha_s)$ reggeised correction *only*. When the ‘correction’ increases, the higher-order α_s terms become important, replacing effectively the first and negative α_s contribution (which we denote $-\delta_R$) by a positive exponential factor like $\exp(-\delta_R)$.

The DPS contribution, which originates from the fusion of gluons from two parton cascades, reveals quite a different behaviour. Due to the growth of the low x gluon density this part of cross section increases with the initial energy and/or with $|Y|$. The DPS mechanism for $\chi_c(1^+)$ production is seen to provide about 30 % of the cross section for $Y = 4$ to 5. At very high energies (asymptotically) this contribution starts to dominate.

The values of the $\chi_b(1^+)$ cross sections are much smaller, but due to the larger χ_b mass the perturbative predictions are better justified. Note also the strong correction caused by gluon reggeisation, which arises since the virtuality of the gluon is larger.

Acknowledgments We are grateful to Jean-Philippe Lansberg for a useful discussion and valuable comments. MGR thanks the IPPP at the University of Durham for hospitality. This work was supported by the RSCF grant 14-22-00281. VAK thanks the Leverhulme Trust for an Emeritus Fellowship.

Open Access This article is distributed under the terms of the Creative Commons Attribution 4.0 International License (<http://creativecommons.org/licenses/by/4.0/>), which permits unrestricted use, distribution, and reproduction in any medium, provided you give appropriate credit to the original author(s) and the source, provide a link to the Creative Commons license, and indicate if changes were made. Funded by SCOAP³.

References

1. L.D. Landau, Dokl. Akad. Nauk ser. Fiz. **60**, 207 (1948)
2. C.N. Yang, Phys. Rev. **77**, 242 (1950)
3. V.A. Khoze, A.D. Martin, M.G. Ryskin, W.J. Stirling, Eur. Phys. J. C **39**, 163 (2005)
4. L. Motyka, M. Sadzikowski, [arXiv:1501.04915](#) [hep-ph]
5. A. Andronic et al., [arXiv:1506.03981](#) [nucl-ex]
6. CMS Collab. (Vardan Khachatryan et al.), Phys. Lett. B **743**, 383 (2015)
7. LHCb Collab. (R. Aaij et al.), JHEP **1310**, 115 (2013). [arXiv:1307.4285](#) [hep-ex]
8. A.K. Likhoded, A.V. Luchinsky, S.V. Poslavsky, Phys. Rev. D **86**, 074027 (2012). [arXiv:1203.4893](#)
9. A.K. Likhoded, A.V. Luchinsky, S.V. Poslavsky, Phys. Rev. D **90**(7), 074021 (2014)
10. E672-E706 Collab. (V. Koreshev et al.), Phys. Rev. Lett. **77**, 4294 (1996)
11. L. Massacrier, B. Trzeciak, F. Fleuret, C. Hadjidakis, D. Kikola, J.P. Lansberg, H.S. Shao, [arXiv:1504.05145](#) [hep-ex]
12. R. Gastmans, W. Troost, T.T. Wu, Phys. Lett. B **184**, 257 (1987)
13. R. Gastmans, W. Troost, T.T. Wu, Nucl. Phys. B **291**, 731 (1987)
14. J.P. Lansberg, J.R. Cudell, Y.L. Kalinovsky, Phys. Lett. B **633**, 301 (2006). [arXiv:hep-ph/0507060](#)
15. H. Haberzettl, J.P. Lansberg, Phys. Rev. Lett. **100**, 032006 (2008). [arXiv:0709.3471](#)
16. P. Artoisenet, E. Braaten, Phys. Rev. D **80**, 034018 (2009). [arXiv:0907.0025](#) [hep-ph]
17. N. Brambilla et al., Eur. Phys. J. C **71**, 1534 (2011). [arXiv:1010.5827](#) [hep-ph]
18. H.S. Shao, Y.Q. Ma, K. Wang, K.T. Chao, Phys. Rev. Lett. **112**(18), 182003 (2014). [arXiv:1402.2913](#)
19. Y.Q. Ma, K. Wang, K.T. Chao, Phys. Rev. D **83**, 111503 (2011). [arXiv:1002.3987](#)
20. D. Diakonov, M.G. Ryskin, A.G. Shuvaev, JHEP **1302**, 069 (2013)
21. V.A. Khoze, A.D. Martin, M.G. Ryskin, Eur. Phys. J. C **23**, 311 (2002)
22. A.D. Martin, W.J. Stirling, R.S. Thorne, G. Watt, Eur. Phys. J. C **63**, 189 (2009)
23. P. Hagler, R. Kirschner, A. Schafer, L. Szymanowski, O.V. Teryaev, Phys. Rev. Lett. **86**, 1446 (2001). [arXiv:hep-ph/0004263](#)
24. C.F. von Weizsacker, Z. Phys. **88**, 612–625 (1934)
25. E.J. Williams, Phys. Rev. **45**, 729–730 (1934)
26. M.A. Kimber, A.D. Martin, M.G. Ryskin, Phys. Rev. D **63**, 114027 (2001)
27. A.D. Martin, M.G. Ryskin, G. Watt, Eur. Phys. J. C **66**, 163 (2010)
28. V.S. Fadin, E.A. Kuraev, L.N. Lipatov, Phys. Lett. B **60**, 50 (1975)
29. L.N. Lipatov, V.S. Fadin, Sov. Phys. JETP **44**, 443 (1976)
30. E.A. Kuraev, L.N. Lipatov, V.S. Fadin, Sov. Phys. JETP **45**, 199 (1977)
31. L.V. Gribov, E.M. Levin, M.G. Ryskin, Phys. Rep. **100**, 1 (1983)
32. M. Ciafaloni, D. Colferai, G.P. Salam, Phys. Rev. D **60**, 114036 (1999)
33. G.P. Salam, JHEP **9807**, 019 (1998)
34. V.A. Khoze, A.D. Martin, M.G. Ryskin, W.J. Stirling, Phys. Rev. D **70**, 074013 (2004)
35. L. Ametller et al., Phys. Lett. B **169**, 289 (1986)
36. L. Frankfurt, M. Strikman, Phys. Rev. D **66**, 031502 (2002)
37. J.H. Kuhn, J. Kaplan, El G.O. Safani, Nucl. Phys. B **157**, 125 (1979)
38. C.D.F. Collab. (F. Abe et al.), Phys. Rev. D **56**, 3811–3832 (1997)
39. D0 Collab. (V.M. Abazov et al.), Phys. Rev. D **81**, 052012 (2010)